infrastructures

MDPI

Review

Design Principles to Reduce Vehicle Pocketing at Guardrail-to-Concrete Barrier Transitions

Desiree Kofler [1,*], Ernst Tomasch [1], Christian Mader [2], Marco Jiraut [2], Alexander Barnaš [3], Olivier Jantscher [3], Johann Horvatits [4] and Karl Gragger [5]

[1] Vehicle Safety Institute, Graz University of Technology, 8010 Graz, Austria; ernst.tomasch@tugraz.at
[2] voestalpine Krems Finaltechnik GmbH, 3500 Krems, Austria
[3] MABA Fertigteilindustrie GmbH, 2752 Wöllersdorf, Austria
[4] Federal Ministry Republic of Austria—Climate Action, Environment, Energy, Mobility, Innovation and Technology, 1030 Vienna, Austria
[5] ASFINAG—Autobahnen-und Schnellstraßen-Finanzierungs-Aktiengesellschaft, 1030 Vienna, Austria
* Correspondence: desiree.kofler@tugraz.at

Abstract: Road restraint systems (RRSs) on European roads are provided by several manufacturers and, hence, lead to differences in geometry, material, and mode of operation. Focusing on the combination of soft steel RRSs with relatively stiffer concrete RRSs, it is vital to consider the potentially critical deformation kinematics during vehicle impacts, such as vehicle pocketing. Since a statutory test procedure was not introduced until mid-2024, much of the transition construction (TC) on Austrian roads has remained untested. Knowledge of the design features to be implemented during the refurbishment of such TCs is of great interest. The main focus of this study was to derive constructive measures (CMs) that increase traffic safety and are applicable to various TCs already installed on roads. The first step involved deriving design principles whose implementations in TCs reduce the risk of critical vehicle or RRS behavior. Based on finite element simulations, the functionality of a TC featuring all derived design principles was examined. The effect of each individual CM was analyzed in a parameter study. The results from a TB61 impact simulation on the derived TC showed the effectiveness of CMs, achieving smooth vehicle redirection. Vehicle pocketing was limited to a minimum, and neither penetration of the TC nor rollover of the vehicle was observed. The analysis of the influence of each CM indicated positive, and in some cases, negative effects. The working width was mainly positively influenced by the compaction of the posts, an additional steel bar, and the chamfering of the first concrete element. A rather diverse picture is drawn regarding the influence on the tensile forces in the guardrails. Some CMs had both positive and negative effects on the distribution of forces in the upper and lower guardrails. Nevertheless, all CMs had positive effects on the tensile forces in the coupling. The chamfering of the first concrete element was the most effective measure to prevent vehicle pocketing. However, through the combination of all CMs, the positive effects predominated, ensuring the functionality of the TC as a whole. This study provides basic insights into the effectiveness of constructive measures, which can serve as a reference for the renovation of in-service TCs or in the development phase of new TCs to be certified.

Keywords: road restraint systems; transition construction; finite element simulation; EN 1317

Citation: Kofler, D.; Tomasch, E.; Mader, C.; Jiraut, M.; Barnaš, A.; Jantscher, O.; Horvatits, J.; Gragger, K. Design Principles to Reduce Vehicle Pocketing at Guardrail-to-Concrete Barrier Transitions. *Infrastructures* **2024**, *9*, 199. https://doi.org/10.3390/infrastructures9110199

Academic Editor: António Couto

Received: 18 September 2024
Revised: 31 October 2024
Accepted: 3 November 2024
Published: 5 November 2024

1. Introduction

The number of single-vehicle accidents in Europe accounts for approximately one-third of all fatal accidents [1]. Approximately 6500 passengers are killed in single-vehicle accidents every year. Two-thirds of these accidents take place on rural roads or motorways [2]. Measures to prevent single-vehicle run-off-road accidents include lane departure warning systems (LDWSs) and lane keeping assist (LKA). The effectiveness of these systems in preventing single-vehicle run-off-road accidents is estimated to be up to 60% [3–5]. Although

the number of vehicles equipped with LDWSs is increasing, only one in five cars in Germany was fitted with an LDWS in 2023 [6,7]. Furthermore, inclement weather conditions and temporarily inconsistent road markings have negative impacts on the effectiveness of these systems [8–10]. Consequently, it is still necessary to provide appropriate measures to protect vehicle occupants from the consequences of collisions with stationary hazards.

Road restraint systems (RRSs) are used to protect errant vehicles from impacts against hazardous objects on the roadside or frontal collisions with oncoming traffic at the median. RRSs are an effective measure and have led to a reduction in the risk of injury [11,12]. To be installed on European roads, RRSs must comply with the criteria specified in EN 1317-2 [13] crash tests. RRSs can mainly be categorized as steel or concrete. Due to various roadside conditions and road safety requirements, several different RRSs are installed on European roads. RRSs are differentiated according to their containment level, which indicates the restraint abilities for particular vehicle classes. The stiffnesses of such systems can be expressed in terms of working width. Due to many different demands, there are a number of certified RRSs in each category, covering a wide range of containment levels and working widths. Therefore, encountering two different RRSs is inevitable.

With regard to connecting two different RRSs (transitions), EN 1317-10 [14], which was published in July 2024, defines crash test configurations and assessment criteria. Due to the fact EN 1317-10 is a preliminary norm since mid-2024, only a small number of transitions tested and certificated according to EN1317 are available and intended for use. Only two transition constructions (TCs) connecting guardrails to concrete barriers are registered in Austria [15]. These transitions are individual constructive solutions adjusted to the local boundary conditions given by the connected RRS and the prevailing environment. Although ENV 1317-10 is used to assess the containment performance of the transition when connecting two new and different RRSs, many different RRSs on the road will never be subjected to an impact test. For these system combinations, however, a sufficiently high level of traffic safety and penetration prevention must be provided.

The main challenge involves the different stiffnesses of the systems to be connected and the prevention of vehicle pocketing. Vehicle pocketing, or a 'knee-shaped' deformation of the softer system, increases the load on the vehicle and supports critical vehicle kinematics [16]. Design measures shall be developed to ensure smooth redirection of the impacting vehicle over the entire length of the transition.

Several studies on road safety have used different methods to investigate the effectiveness of design measures for steel and concrete barriers. The calculations of numerical risk factors and cost-benefit analysis, as conducted by [17], provide insight into critical road infrastructure on a macroscopic basis. However, in order to investigate factors influencing the detailed construction and design of roadside barriers, investigations focusing on vehicle kinematics and vehicle-infrastructure interaction are essential. For this purpose, finite element (FE) simulations are widely used and significantly advance crashworthiness analysis. By validating FE simulation models with real crash test data, reliable models can be established [18]. As field data often deviate from test standards [19], FE simulations provide a cost-effective method to evaluate the behavior of barriers in impact configurations different from those addressed in regulatory-required tests. In addition, parameter studies provide a deeper understanding of the influence of design parameters such as material failure, friction, and geometric design on restraint functionality [20].

The objective of this study is to analyze design principles and derive design measures to improve the restraint functionality of TCs and to prevent vehicle pocketing when connecting two different RRSs, specifically when connecting a guardrail to a concrete barrier. A parameter study of a virtually optimized and tested TC based on two representative RRSs shows the benefits of each design measure implemented. Based on the relative comparisons, recommendations are made regarding the need for adjustments to the TC in service. Ultimately, the design measures are universally applicable and can be applied to combinations of RRSs not investigated in this study.

2. Materials and Methods

The approach to evaluating the restraint potential of constructive measures (CMs) is processed in three steps (Figure 1). Based on the literature, restraint principles of existing TCs were derived, and CMs for implementing each principle in a TC were developed. A finite element (FE) model of a TC is introduced, combining models of a steel RRS and a concrete RRS validated for H3 and H4b containment levels, respectively. The TC is designed using all derived CMs. The functionality and restraint capabilities of the TC are evaluated by conducting a simulation of the certification test TB61 according to EN 1317-2 [13]. Furthermore, the extent to which each single constructive measure contributes to the restraint capability of the TC is analyzed by a parameter variation.

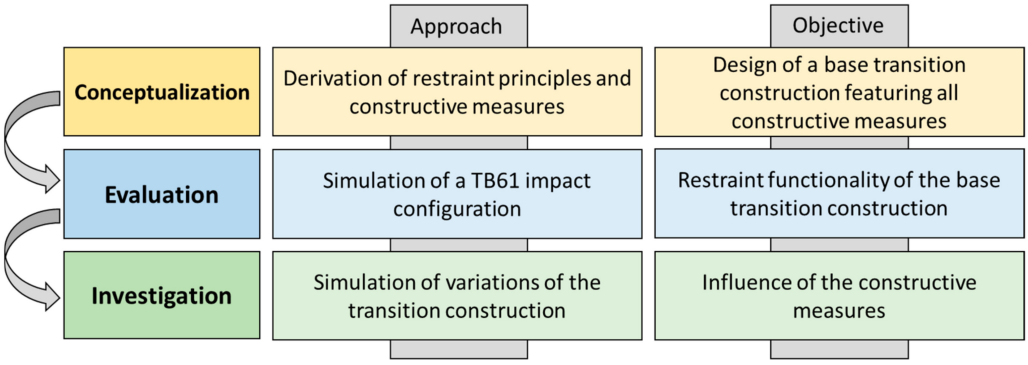

Figure 1. Approach to evaluating the influence of restraint principles.

2.1. Restraint Principles and Constructive Measures

For a TC to address the restraint functionality for passenger cars and heavy goods vehicles, the following restraint principles are implemented:

- RP1: Gradually increase the stiffness from the (softer) guardrail toward the (stiffer) concrete barrier.
- RP2: Increase the stiffness of the RRS to counteract the potential penetration of the TC caused by the impact of a heavy goods vehicle. This can be achieved by reinforcing the tension belt, such as installing a second steel profile on the non-traffic side of the guardrail.
- RP3: Extend or reinforce the anchorage, i.e., increase the number of anchoring posts or integrate posts with increased cross-sectional resistance, which contributes to the stiffness characteristics.
- RP4: Extend the deformation space to reduce the stiffness difference between the guardrail and concrete barrier and smoothly redirect the vehicle.
- RP4: Prevent vehicle pocketing in the first concrete barrier elements in order to reduce severe passenger loads or critical vehicle kinematics.

To apply these identified restraint principles in the TC concept, CMs were developed and implemented in the TC. Existing TCs connecting steel and concrete RRSs were analyzed with respect to the restraint principles. In Table 1, the CMs implemented in the TCs are associated with the restraint principles (RPs).

Figure 2 illustrates the realization of the CM in a TC. An increase in stiffness from the guardrail toward the concrete barrier is realized by increasing the number of posts of the guardrail (CM1). A second guardrail bar (upper guardrail) reinforces the tension belt. Three fixation posts were installed to connect the upper guardrail to the connection element (CM2). By positioning the concrete elements with a lateral offset and installing steel damping parts between the guardrail and the concrete barrier elements, the deformation space increases (CM3 and CM4). Hence, the connection element is activated earlier and energy can be absorbed through the deformation of the damping parts. The second concrete element is rotated around the height axis to ensure the alignment of the other concrete barriers with the traffic face of the RRS. To prevent vehicle pocketing, an additional steel bar

(sliding profile) is mounted at the bottom of the guardrail and is anchored in the connection element (CM5). The last post of the steel RRS is positioned relative to the connection element with minimal post distance, which prevents vehicle pocketing (CM6). A special design shape of the first concrete barrier element (connection element), referred to as a chamfered front face, will further reduce the risk of vehicle pocketing (CM7).

Table 1. Restraint principles and corresponding constructive measures.

Restraint Principles		Constructive Measures	
RP1	Increase stiffness gradually from the guardrail to the concrete barrier	CM1	Gradually increase the number of posts toward the concrete barrier
RP2	Reinforce the tension belt	CM2	Fix the second guard rail to the concrete barrier elements
RP3	Extend or reinforce the anchorage	CM1	Gradually increase the number of posts toward the concrete barrier
RP4	Extend the deformation space	CM3	Damping steel parts between the guardrail and concrete barrier element
		CM4	Offset the first concrete barrier element

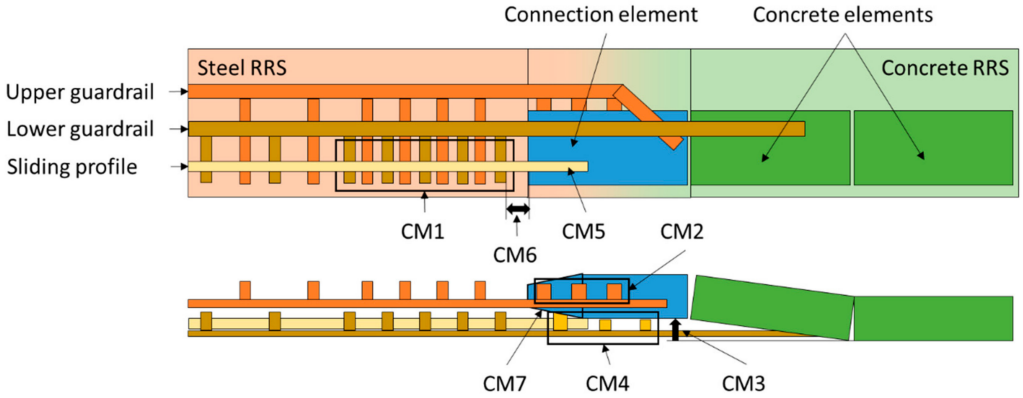

Figure 2. Schematic illustration of the constructive measures.

2.2. Finite Element Model and Validation of the RRS

Two RRSs were chosen for this study due to their frequent use on Austrian motorways: the steel RRS KB1 RH3 from voestalpine Krems Finaltechnik GmbH and the concrete RRS DB100 6m from DELTABLOC GmbH. The steel RRS is certificated according to EN 1317-2 [13] for containment level H3 with a working width of W5, and the concrete RRS for containment level H4b with a working width of W6. Both RRSs are approved for use on Austrian roads and registered by the Ministry of Transport [15]. These two RRSs are used as the base RRSs, which are connected by a TC. This TC is referred to as the base TC and includes the above-mentioned CMs.

2.2.1. Road Restraint Finite Element Model

FE models of the base RRS were set up and validated against data from tests. The FE simulations were performed using LS-Dyna solver R9.3.1 MPP double precision (LSTC, Livermore, CA). In Figure 3, the FE models of one segment of the guardrail and the concrete barrier are shown. The entire model of each RRS is put together with the same number of segments as in the corresponding tested configuration.

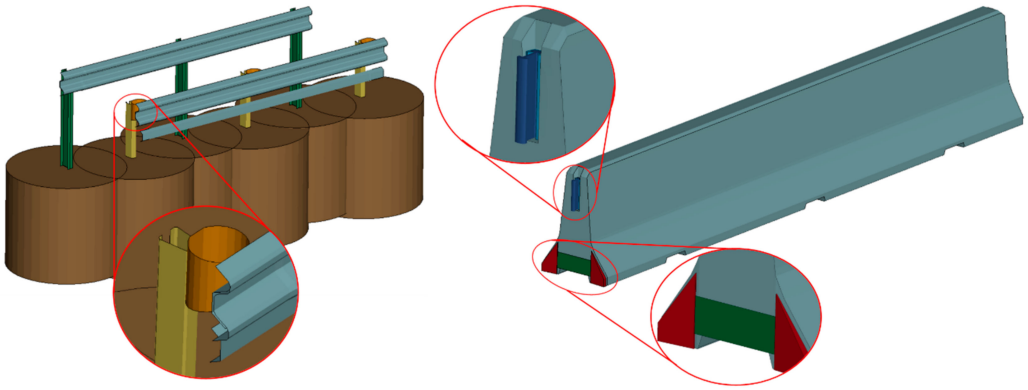

Figure 3. Models of the base RRS KB1 RH3 (**left**) and DB100 6m (**right**).

The steel RRS consists of two independent guardrails and is modeled with shell elements and elastic–plastic steel material properties. Bolt connections that link the guardrails (gray) with the damping elements (orange) and the posts (yellow/green) were simplified via beam elements with mechanical characteristics as the corresponding bolts. The posts were embedded in solid elements (brown) representing the soil. The material parameters and the modeling method for the soil were taken from the literature [21]. Both free ends of the RRS were fixed in space to represent the start and end anchorages.

The concrete barrier was modeled with rigid solid elements (gray), as no deformation or damage was observed in the test data. The coupling and connector parts (blue) were modeled with solid elements and allocated with elastic–plastic steel material properties. The couplings on both free ends of the RRS were fixed in space to represent the start and end anchorages. In between each concrete element, two wedges (red) with elastic–plastic material properties, connected by a rubber strap (green), were positioned.

2.2.2. Validation of the Road Restraint Models

For an RRS to be considered valid, it must successfully complete two different tests [13]. For containment level H3, a test with a vehicle mass of 900 kg, an impact speed of 100 km/h, and an impact angle of 20° is required. This test is referred to as TB11. A second test with a heavy goods vehicle with a mass of 16,000 kg, an impact speed of 80 km/h, and an impact angle of 20° is mandatory. This test is referred to as TB61. For containment level H4b, the TB11 test is mandatory, and a further test with a heavy goods vehicle with a mass of 38,000 kg, an impact speed of 65 km/h, and an impact angle of 20° is required. This test is referred to as TB81. The corresponding test reports and technical drawings for the validation are provided by the manufacturer. The impact angle, impact velocity, impact position, and vehicle properties—such as mass and position of the center of gravity—are modeled as given by the test reports and in accordance with the test specifications of EN 1317-2 [13].

The validity of the models is based on EN 16303 [22]. The tolerance limits for the deformation of the RRS, such as dynamic deflection (Dm), working width (Wm), vehicle intrusion (VIm), and the severity criteria—Acceleration Severity Index (ASI) and Theoretical Head Impact Velocity (THIV)—defined therein are met by the simulations. Table 2 summarizes the evaluation criteria, which are fulfilled according to EN 16303 [22] for the individual impact configurations and RRSs.

Table 2. Impact configurations and evaluation criteria of the validated RRSs.

RRS	TB11	TB61	TB81
VAKF KB1 RH3	Dm/Wm/ASI/THIV	Dm/Wm/VIm	-
DELTABLOC DB100	Dm/Wm/ASI/THIV	-	Dm/Wm/VIm

In further investigations, the validated steel RRS is referred to as the base steel RRS, and the validated concrete RRS is referred to as the base concrete RRS.

2.2.3. Model of the Base TC

The base TC is shown in Figure 4 with the base steel and base concrete RRS on the left and right sides, respectively, colored brown. All of the identified restraint principles are considered, and appropriate CMs are applied. The base TC connecting the modified steel and concrete RRS (green) via a connection element (blue) is outlined. The connection element is modeled with elastic–plastic concrete material properties and includes steel reinforcement bars that are also modeled with elastic–plastic material properties.

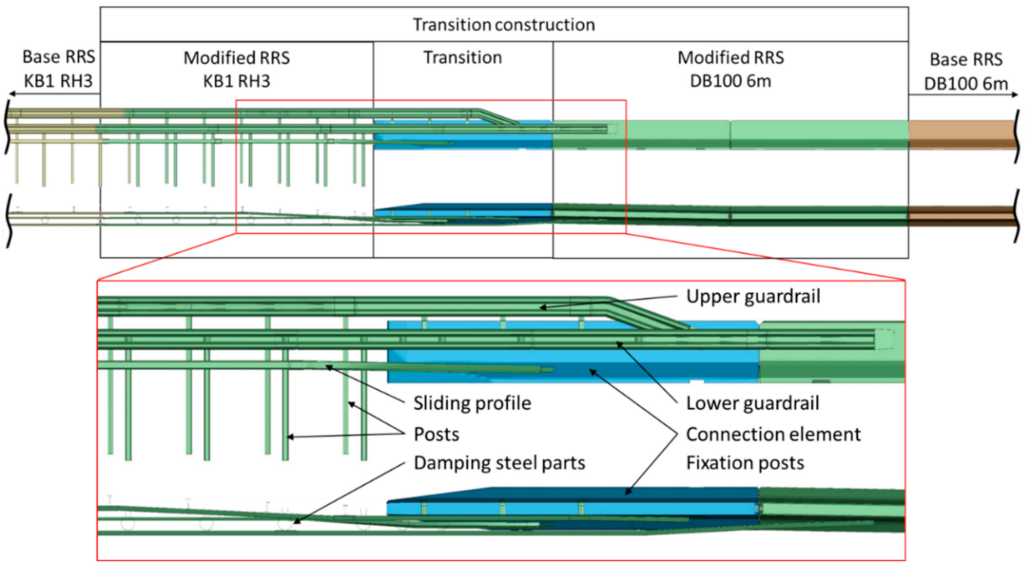

Figure 4. Model of the base transition construction.

2.3. Influence of the Constructive Measures

The functionality of the base TC is evaluated for the TB61 impact scenario at three different impact locations. Furthermore, the most critical impact location is identified. To evaluate the influence of the implemented CMs, a parameter study was conducted for the TB61 impact scenario in the most critical impact location. Several variations of the base TC were set up, with each variation reduced by one of the implemented CMs. A comparison between the results of the base TC and the variations provides insight into the influences of each constrictive measure.

2.3.1. Vehicle Model

The TB61 configuration involves the impact of a 16 t heavy goods vehicle traveling at 80 km/h and an impact angle of 20°. The FE model (Figure 5) is based on a freely available vehicle model from the NCAC [23].

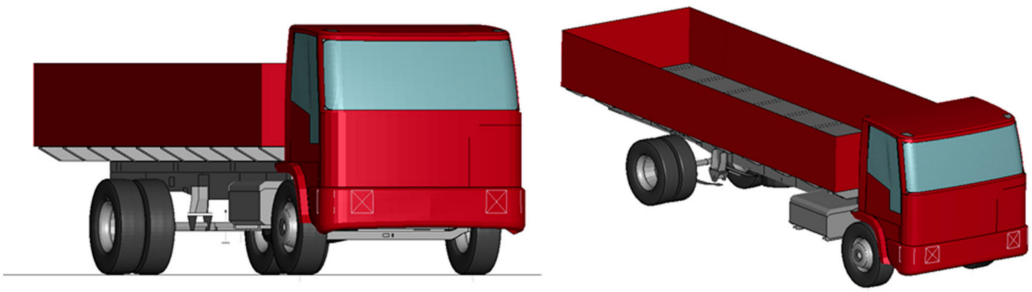

Figure 5. FE model of the heavy goods vehicle.

The model includes a geometrical representation and features air-filled tires, a suspended and steerable front axis, and a suspended rear axis equipped with dual tires.

Despite the motor block and parts included in joints, all parts are modeled with deformable materials. Bolt connections are simplified via nodal rigid body constraints. Modifications were made to the original suspension characteristics to enable improved vehicle–barrier interaction. The major characteristics of the model are listed in Table 3.

Table 3. Characteristics of the FE model of the heavy goods vehicle.

Characteristic	Value
Length [m]	9.40
Width [m]	2.49
Height [m]	2.76
Number of parts	181
Number of nodes	70,510
Number of elements	82,862

2.3.2. Impact Location

EN 1317-10 [14] provides guidance on defining the impact location for containment tests as follows: "The impact point for the containment test can be located at the midpoint of the transition but should not be more than 6 m upstream from the end of the transition". However, the regulation also allows for selecting other impact points if the proposed location is not considered the worst case. The impact location, as defined by the regulation, would be within the concrete elements. As vehicle pocketing in the steel RRS is expected to be the most critical loading scenario due to lateral stiffness variations between the softer steel and stiffer concrete RRSs, impact locations outside the recommendations of the regulation are selected.

The impact locations in Figure 6 were chosen, assuming that one of them represents the most critical loading scenario for the TC. Impact locations A and B are situated on the seventh and fourth posts of the upper guardrail, which are located 8260 mm and 4460 mm before the connection element, respectively. Impact location C is situated at the second post of the lower guardrail, which is 1640 mm before the connection element.

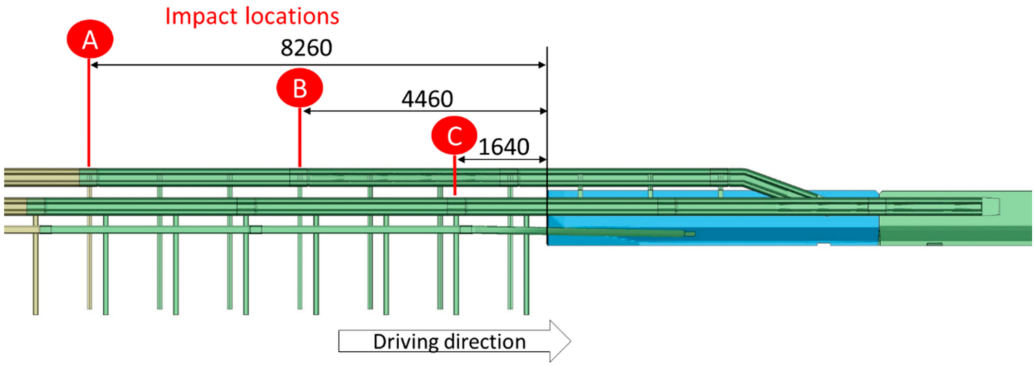

Figure 6. Impact location for the evaluation of the transition construction.

2.3.3. Model Variations of the Base TC

Based on the base TC and all the CMs taken into consideration therein, a variation study with a total of seven variations of the base TC (V1 to V7) was conducted. For each variation, one of the implemented measures (CM1 to CM7) was removed (CM1 was removed in V1, CM2 was removed in V2, and so on). By comparing the simulation results between the base TC and each variation, the influence of each constructive measure can be identified. The following variants were analyzed:

V1: No compaction of post distance: CM1 was removed from the base TC by resting the post distance in the modified steel RRS to the post distance of the base steel RRS. For the used steel RRS, this meant an increase in post distance from 1.267 m to 1.9 m in the last 8 m before the connection element (Figure 7).

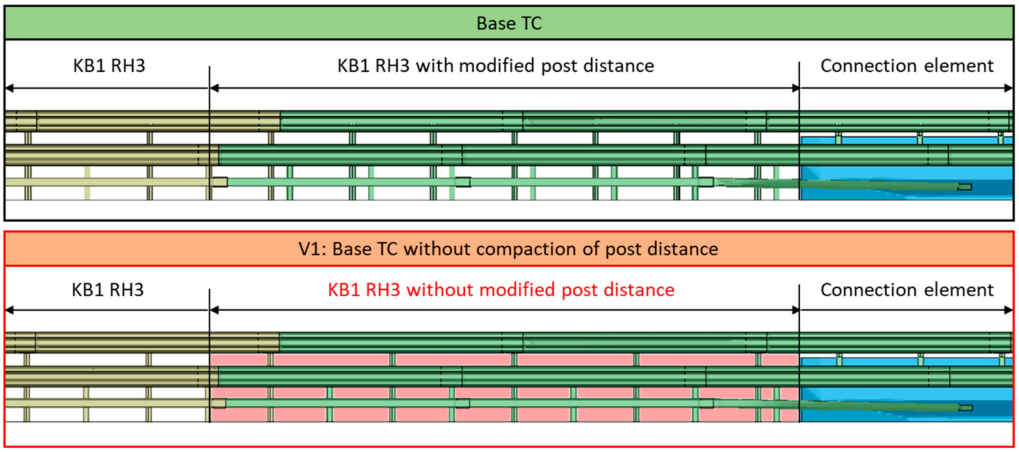

Figure 7. Base TC and TC modification V1.

V2: Fewer fixation posts between the upper guardrail and the concrete element: By implementing CM2, the base TC included three fixation posts to connect the upper guardrail to the connection element. In this variation, the number of posts was reduced to two (Figure 8).

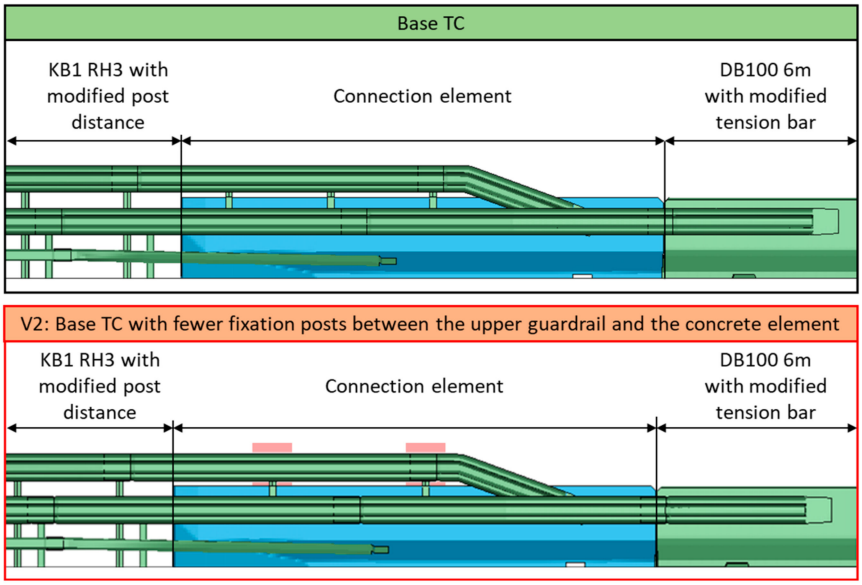

Figure 8. Base TC and TC modification V2.

V3: No damping steel parts between the guardrail and concrete element: The damping steel parts between the connection element and the steel guardrail installed in the base TC, based on CM3, were removed in this modification (Figure 9).

V4: No lateral offset of the first concrete elements: The lateral offset of the first concrete elements included in the base TC, addressing CM4, was removed by resituating all concrete elements to align with the line of the traffic face of the RRS. Due to the resulting decrease in lateral distance between the connection element and the steel guardrail, the damping steel parts needed to be replaced with more compact damping elements from another steel RRS of the same manufacturer (Figure 10).

V5: No additional steel bar at the bottom, referred to as a sliding profile: The sliding profile, which was integrated into the base TC based on CM5, was removed in this modification (Figure 11).

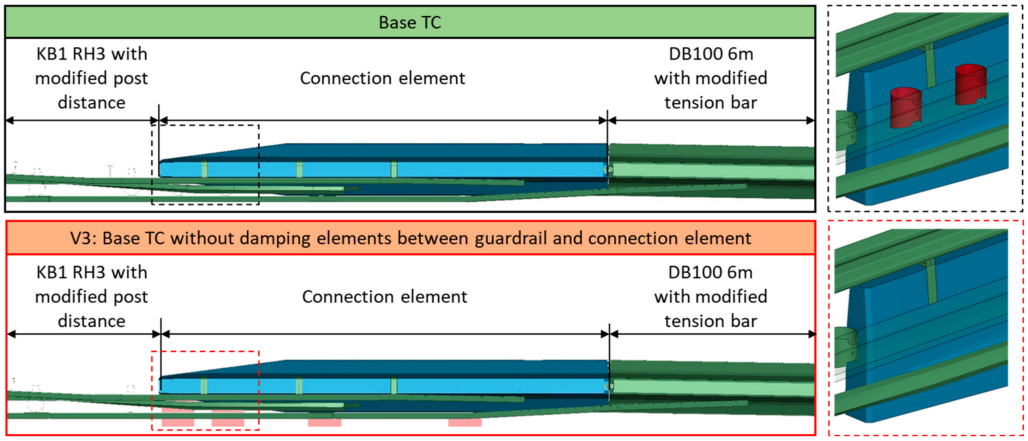

Figure 9. Base TC and TC modification V3.

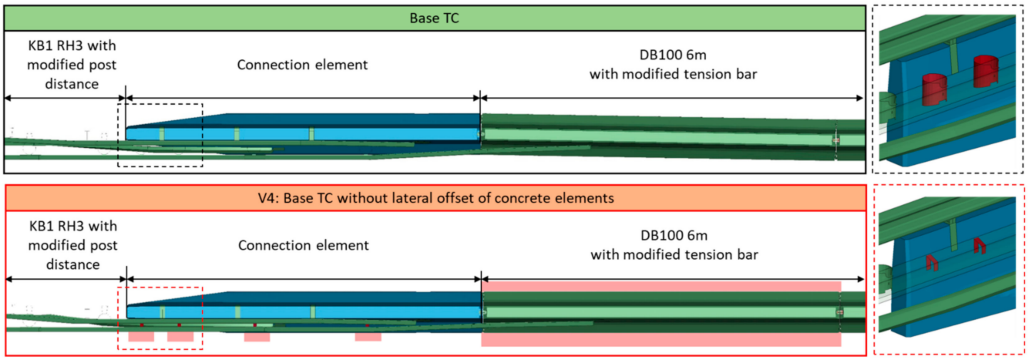

Figure 10. Base TC and TC modification V4.

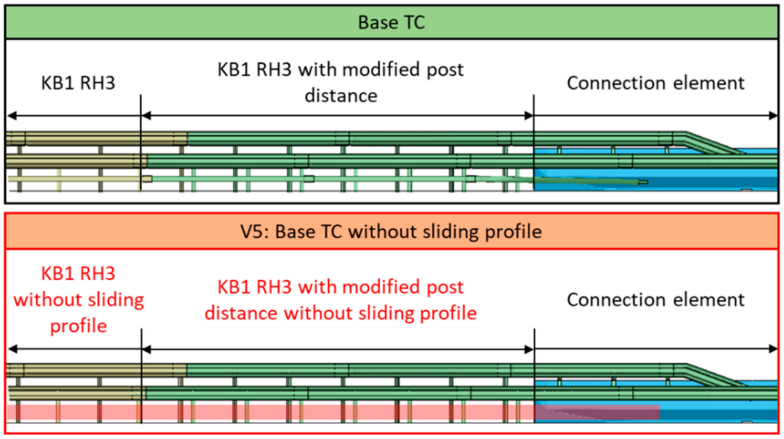

Figure 11. Base TC and TC modification V5.

V6: Greater distance between the last post and concrete barrier element: To remove CM6 from the TC, the distance between the last post of the steel RRS and the connection element was increased by removing the last post. For the steel RRS used, this meant an increase in the distance from 0.35 m to 1.617 m between the last post and the front face of the connection element (Figure 12).

V7: No chamfering of the front face of the connection element: The chamfering of the connection element (CM7) was removed by modifying the geometry to resemble the geometry of a standard concrete element. Thereby, inner reinforcements were kept the same as in the connection element (Figure 13).

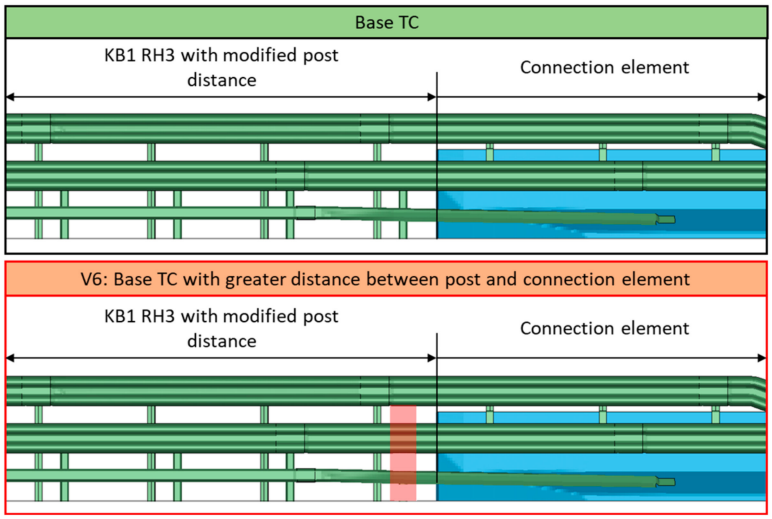

Figure 12. Base TC and TC modification V6.

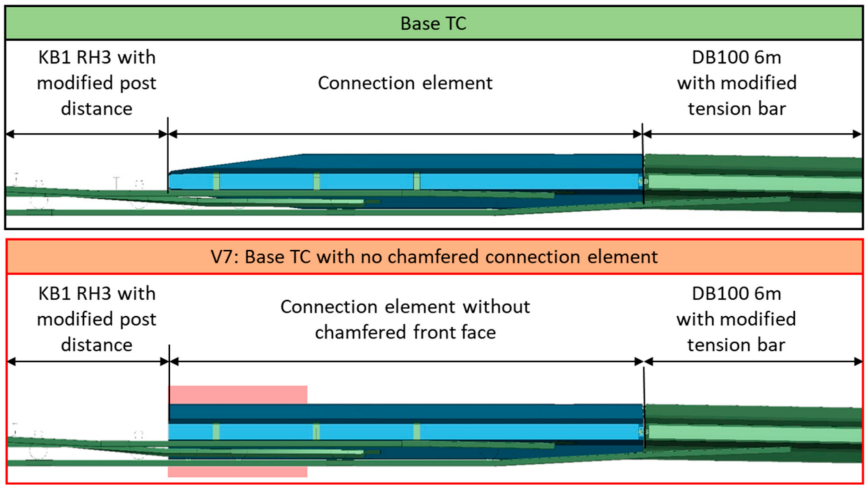

Figure 13. Base TC and TC modification V7.

2.3.4. Effectiveness Assessment

The restraint capability of the TC was evaluated by comparing the maximal tensile force measured in the simulation and the comparative values provided by the manufacturers. Moreover, a comparison of the different simulation variations with the base TC was also conducted by means of the measured tensile forces. To do so, the FE model was equipped with time history outputs. Tensile force measurements in the cross-section of the steel guardrails and the shaft of the connectors for the concrete element couplings were implemented via a *DATABASE_CROSS_SECTION_SET, as illustrated in Figure 14. All couplings and guardrails in the model were equipped with such measurements. For the assessment of the different variations, the maximal values are compared.

As there is no known definition of how to express vehicle pocketing in figures, a method to detect or even quantify vehicle pocketing by applying two approaches is introduced. For the first approach, the contact force is evaluated between the left front wheel and the connection element. If contact occurs, this may indicate poor restraint functionality of the guardrail, which could lead to vehicle pocketing. For the second approach, the tire pressure of the left front wheel is monitored, and if there is an increase in tire pressure, it is assumed that vehicle pocketing may occur. In addition, the working widths of the base TC and all TC variations are measured and compared. Finally, the following four assessment criteria are evaluated:

- Maximal tensile force in the guardrail;
- Maximal tensile force in the coupling;
- Vehicle pocketing;
- Working width.

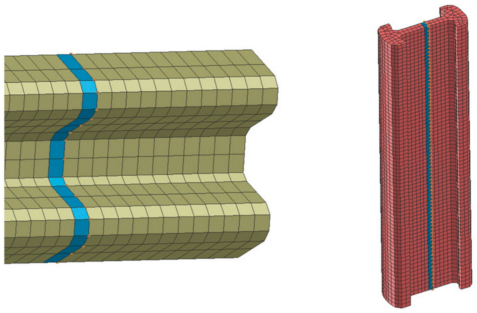

Figure 14. Tensile force measurement cross-sections implemented in the guardrails (**left**) and couplings (**right**).

3. Results

In the following, the results of the simulations with the base TC at the three impact locations and the different variations of the base TC are discussed.

3.1. Evaluation of the TB61 Impact on the Base TC

The FE model of the base TC was set up and simulated for the TB61 impact configuration at the three different impact locations (ILs). At IL A, the vehicle was redirected by the guardrail and did not contact the connection element. Hence, no critical behavior of the TC was assumed. At IL C, the vehicle impacted the connection element and was redirected by it. Therefore, no extensive deformation of the guardrail was noted. The greatest extent of guardrail deformation, which could lead to vehicle pocketing, was observed at IL B, where the guardrail bent outwards in front of the edge of the connection element. A comparison of working widths also supports the argument of IL B being the most critical impact location, as the highest working width is observed here at 1725 mm (Figure 15).

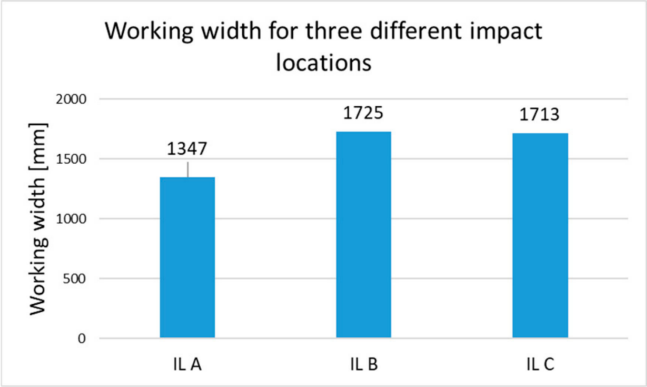

Figure 15. Working width for three different impact locations.

Figure 16 shows the kinematics of the heavy goods vehicle and the system behavior at the IL B in time steps of 200 ms. Neither a rollover nor a penetration of the restraint system at the transition is observed. The measured tensile forces in the couplings and the steel guardrails were compared with the reference values provided by the manufacturers. With the measured values not exceeding the reference values at all three impact locations, the functionality of the base TC was approved.

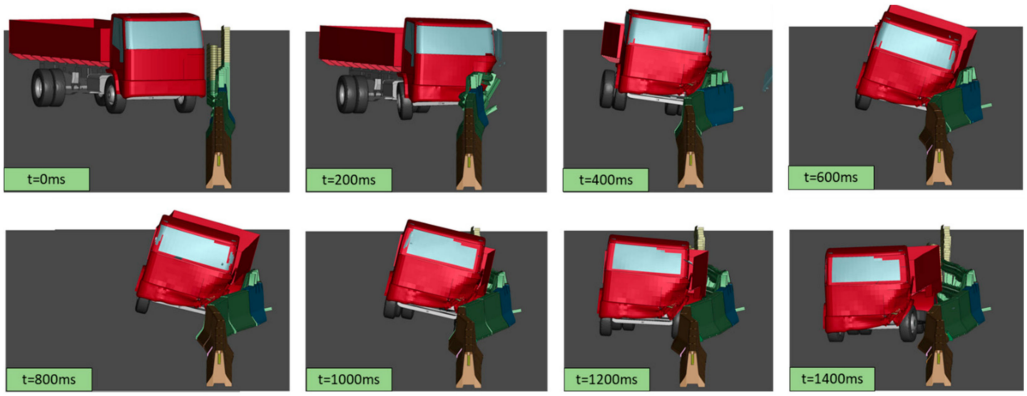

Figure 16. Kinematics of the TB61 impact on the base TC.

3.2. Evaluation of the Influence of Constructive Measures

In the base TC, several CMs were implemented to guarantee functionality for the TB61 impact. In order to investigate the influence of each measure, seven variations (V1 to V7) of the base TC were set up and simulated with the same impact conditions.

Table 4 summarizes the relative deviations in working width, the tensile forces in the guardrails and couplings, and the tire pressure in the front left wheel with respect to the base TC, which results when a certain CM is not implemented. The contact between the connection element and the front left wheel force is given in absolute values, as no relative comparison is possible due to no contact occurring in the simulation with the base TC. The coloring scheme indicates the highest increase in yellow and the highest decrease in blue for each criterion quantified with relative values. The same coloring also applies to the contact forces, highlighting the highest force in yellow and no contact force in blue.

Table 4. The relative deviation of the criteria and absolute contact force in the different TC modifications.

TC Modification	Working Width [%]	Tensile Force in Lower Guardrail [%]	Tensile Force in Upper Guardrail [%]	Tensile Force in Coupling [%]	Wheel Pressure [%]	Contact Force [kN]
V1: No compaction of post distance	13.0	21.2	0.3	9.6	0.3	0.0
V2: Fewer fixation posts between the upper guardrail and the concrete element	6.0	6.5	7.1	6.0	1.7	14.6
V3: No damping steel parts between the guardrail and concrete element	8.7	29.0	−10.4	1.3	0.4	4.3
V4: No lateral offset of the first concrete elements	−1.6	9.4	−4.5	7.3	2.2	10.6
V5: No additional steel bar at the bottom, referred to as a sliding profile	15.3	22.9	4.7	8.9	1.1	3.0
V6: Greater distance between the last post and concrete barrier element	5.9	1.2	−6.2	5.2	−0.5	0.0
V7: No chamfering of the front face of the connection element	12.5	4.1	0.0	4.3	1.0	52.0

The main findings for each variation are discussed in the following sections accompanied by figures. Each figure contains two images: the left image represents the validated base TC as a reference, while the right image shows the results of the variation.

3.2.1. V1: No Compaction of Post Distance

Variation V1, where the CM1 was removed, provides less resistance to lateral deflection due to the smaller number of anchoring posts. Hence, the comparison of the system behavior in Figure 17 shows an increased working width of V1 when compared with the base TC. The working width of the base TC is indicated by the length of the yellow bar, to which a red bar is added, indicating the increase in V1. The working width in V1 increases by 13% (Table 4), which leads to higher tensile forces in the lower guardrail (+21.2%) and in the couplings (+9.6%). Almost no influence on the tensile force in the upper guardrail (+0.3%) is noted. As no contact between the wheel and the connection element is detected

(0.0 kN), and the tire pressure only increases by 0.3%, CM1 is assumed to have no effect on vehicle pocketing behavior.

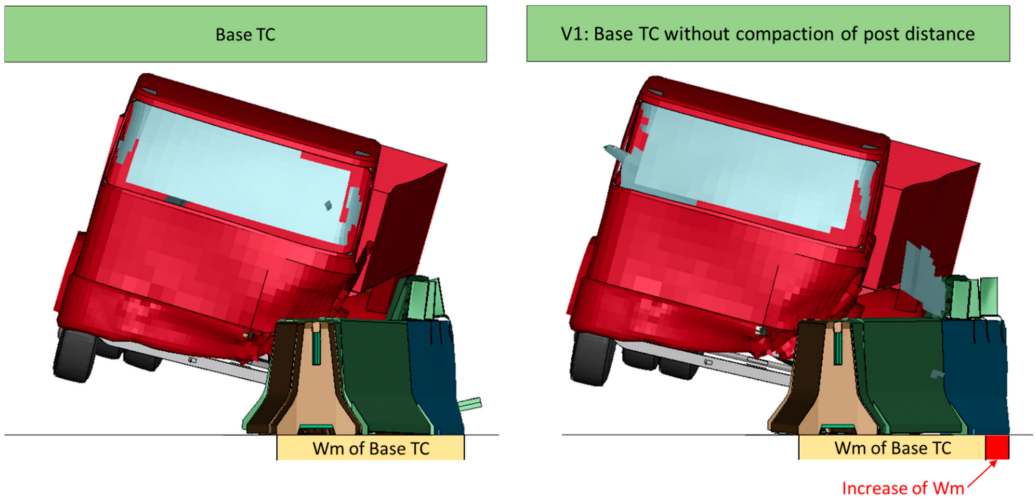

Figure 17. Comparison of the kinematics between the base TC and TC (V1).

3.2.2. V2: Fewer Fixation Posts Between the Upper Guardrail and the Concrete Element

The modification of the fixation posts from three posts in the base TC (featuring CM2) to two posts in the modified TC (V2) results in a 6% increase in the working width (Figure 18, Table 4). The tensile force in the couplings increases by 6.0%, while the forces in the lower and upper guardrails increase by 6.5% and 7.1%, respectively. A contact force of 14.6 kN is detected between the front left wheel and the connection element. Considering the effect of an increased tire pressure percentage of 1.7%, an increased risk of vehicle pocketing is derived for a TC not featuring CM2.

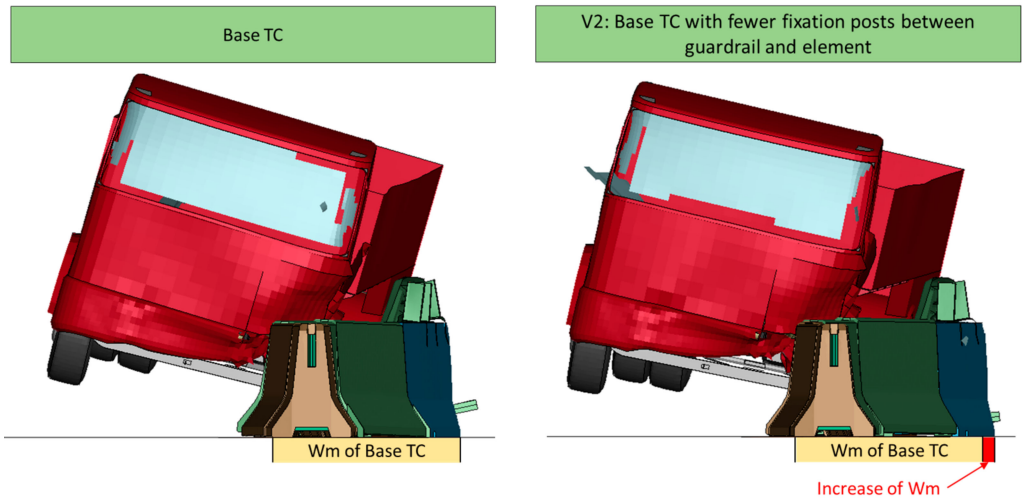

Figure 18. Comparison of the kinematics between the base TC and TC (V2).

3.2.3. V3: No Damping Steel Parts Between the Guardrail and Concrete Element

The damping elements that fix the guardrail at a distance to the connection element in the base TC (CM3) facilitate smoother bending of the guardrail. Without damping elements, the guardrail contacts the connection element and bends outwards in front of the edge of the connection element (Figure 19). With no damping elements installed in the modified TC, the tensile force in the lower guardrail increases by 29% (Table 4). In contrast, the tensile force decreases by 10.4% in the upper guardrail. The working width increases by 8.7% and the tensile force in the couplings increases by 1.3%. Without the damping elements, a

higher risk of vehicle pocketing can be observed based on the detection of contact between the wheel and the connection element (4.3 kN) and an increased tire pressure (+0.4%).

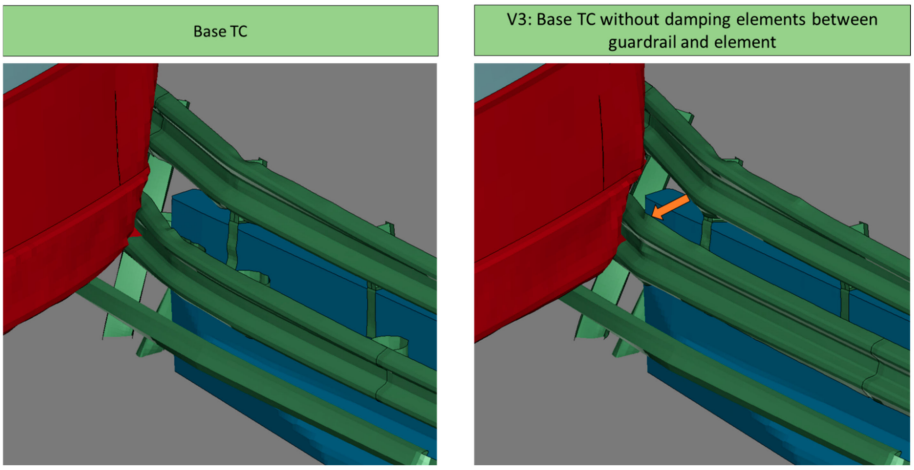

Figure 19. Comparison of the kinematics between the base TC and TC (V3).

3.2.4. V4: No Lateral Offset of the First Concrete Elements

Similar behavior, as observed in V3, is noted in V4 (Figure 20). Without an offset of the first concrete barrier element, the guardrail tends to bend outward more at the connection element compared to the base TC. The increased tire pressure (+2.2%) and the contact force (4.3 kN) indicate an increased risk of vehicle pocketing, which can lead to higher loads on the material. The tensile force in the lower guardrail increases by 9.4% with a lateral offset of the first concrete elements, with the tensile force in the upper guardrail decreasing by 4.5% (Table 4). In addition, the tensile force in the couplings increases by 7.3%.

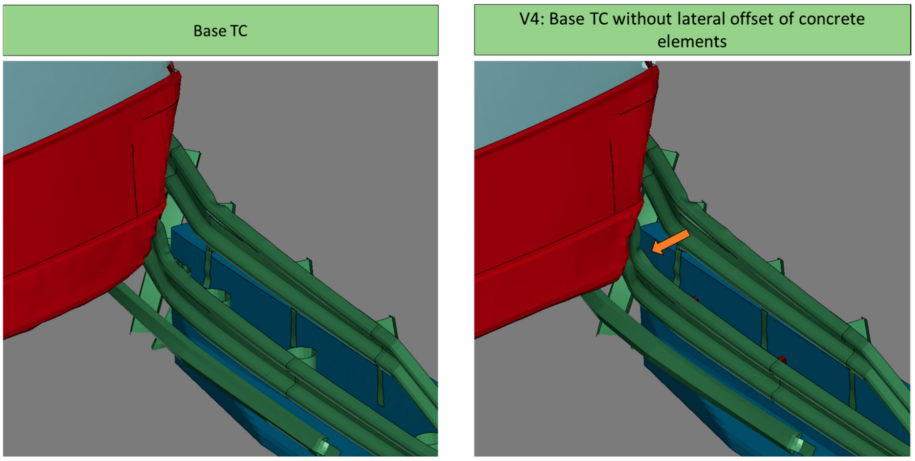

Figure 20. Comparison of the kinematics between the base TC and TC (V4).

3.2.5. V5: No Additional Steel Bar at the Bottom, Referred to as a Sliding Profile

The omission of the sliding profile, which was initially implemented based on CM5, does not influence the vehicle kinematics. Only a change in the deformation of the post closest to the connection element is observed due to the direct contact of the front left wheel with the post (Figure 21). This results in an increased tire pressure of 1.1% (Table 4). In addition, contact between the wheel and the connection element is observed (3.0 kN). Nevertheless, the sliding profile contributes to the lateral resistance of the RRS, which can be seen by a 15.3% increase in working width in the modified TC. The increased deflection further leads to an increase in tensile force in the lower and upper guardrails by 22.9% and 4.7%, respectively. In addition, an increase in the coupling force is observed (8.9%).

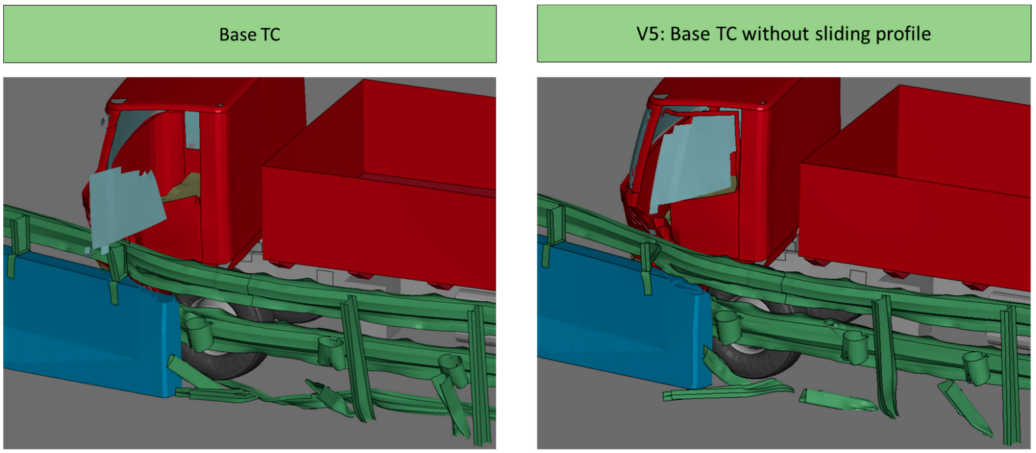

Figure 21. Comparison of the kinematics between the base TC and TC (V5).

3.2.6. V6: Greater Distance Between the Last Post and Concrete Barrier Element

With the last post of the guardrail removed to evaluate the influence of CM6, a reduction in the stiffness of the TC is observed, resulting in a 5.9% increase in working width (Table 4). The tensile force in the lower guardrail shows only minor changes (+1.2%). The tensile force in the upper guardrail decreases by 6.2% and increases by 5.2% in the coupling. Figure 22 shows the interaction between the post near the connection element and the left front wheel in the base TC. No contact between the wheel and the connection element (0.0 kN) is observed, with only a minor change in tire pressure (−0.5%).

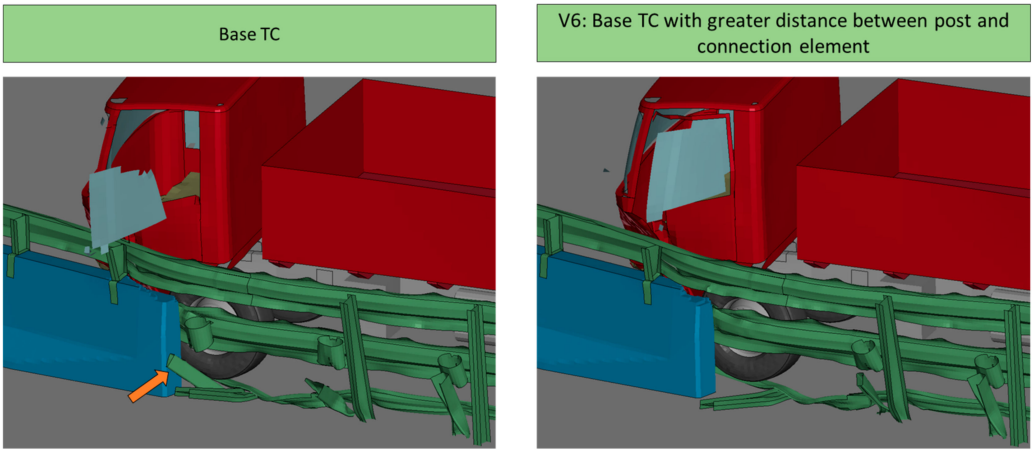

Figure 22. Comparison of the kinematics between the base TC and TC (V6).

3.2.7. V7: No Chamfering of the Front Face of the Connection Element

The influence of the geometry of the connection element (CM7) on the vehicle–RRS interaction can be seen in Figure 23. Without chamfering of the connection element, the left front wheel of the vehicle hits the front flat face of the connection element, leading to vehicle pocketing. This finding can be supported by a measured contact force of 52 kN, and an increase in tire pressure of 1%. With this contact occurring in the modified TC, the working width increases by 12.5% (Table 4). Furthermore, the tensile force in the lower guardrail increases by 4.1%, whereas no change is observed for the upper guardrail. An increase of 4.3% of the tensile force in the coupling is observed.

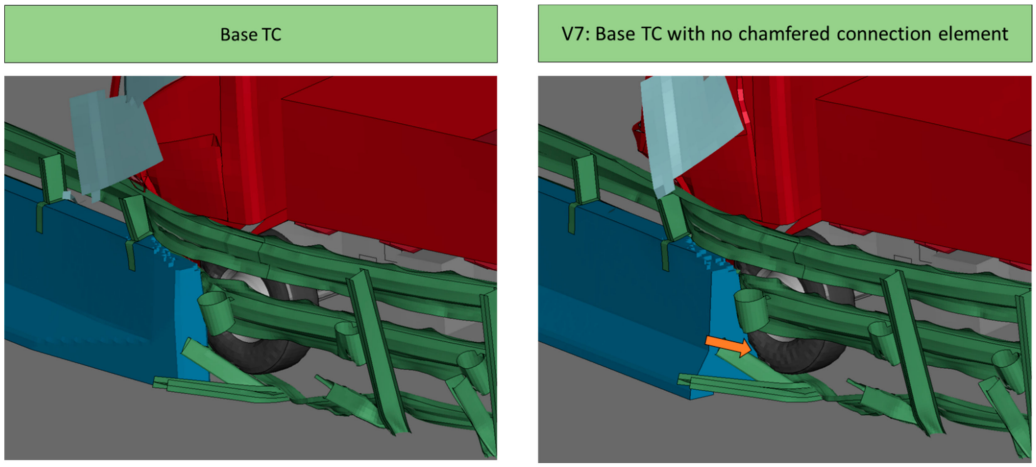

Figure 23. Comparison of the kinematics between the base TC and TC (V7).

4. Discussion

Although there is an increasing trend toward lane departure warning systems in vehicles [6,7], many vehicles are still not equipped with this safety system. RRSs are, therefore, still necessary to protect an errant vehicle from hitting a dangerous obstacle. These RRSs are tested in accordance with the requirements of EN 1317-2 [13], but the transition between two different RRSs is rarely tested because the test standard for transitions (EN 1317-10 [14]) was not published until July 2024. The design and functionality of the TC with the test standard in effect will be evaluated in the future. With more test data being available for different containment levels, the results found in simulation studies can be reviewed and additional constructive measures can be developed.

With no tested TC available for each RRS combination, the large number of different RRSs poses a major challenge. This applies to both new TCs, particularly those that have already been installed on roads and are no longer being tested. This requires practical solutions that increase road safety and can be used for many different RRS combinations.

In this study, a standard TC was developed, and various measures to improve penetration safety and vehicle pocketing were evaluated. In the developed base TC, all CMs were implemented. By simulating the TB61 impact configuration, the functionality of the base TC and, thereby, the performance of the collaboration of all implemented CMs could be approved. For the parameter study, seven variations of the base TC were created, with each one omitting one specific measure. Hence, the results reflect the effect of that specific CM on the behavior of the TC.

The working width was mainly positively influenced by the compaction of posts (CM1) and an additional steel bar (CM5). Those CMs increase the stiffness of the steel RRS and, therefore, provide more resistance to lateral deformation. They also contribute to a smooth and monotonous increase in the stiffness of the whole TC. The geometrical modification, such as the chamfering of the first concrete element (CM7), also reduces the working width of the TC. A negative effect on working width was only documented for the lateral offset of the first concrete element (CM4). However, as the initial position of the connection element is closer to the system's leading edge—where the working width is measured—the comparison of this CM with other variations should be interpreted with care.

A rather diverse picture is drawn regarding the influence on the tensile forces in the guardrails. The implementation of steel damping elements (CM3), the lateral offset of the first concrete element (CM4), and the distance between the last post and the concrete element (CM6) show positive and negative effects on the distribution of forces in the upper and lower guardrails. While the tensile force is reduced in one guardrail, compensation is observed in the other guardrail. Despite these exceptions, an overall positive trend in the influence on tensile forces was observed.

All CMs showed a positive effect on tensile forces in the couplings. A comparable trend of reduction in working width and tensile forces in the couplings was observed, except for CM4, where the above-discussed limitation applies.

There is no straightforward evaluation method to detect vehicle pocketing in FE simulations. The approach taken here facilitated the quantification of the event of vehicle pocketing by evaluating tire pressure and the contact force between the front left wheel and the connection element. Both criteria show either a positive or a negative trend for each CM, indicating a good correlation between both evaluation methods. Only a minor decrease in the wheel pressure was noted for CM1, which could not be reproduced in the contact force criteria. The chamfering of the first concrete element proved to be the most effective measure to prevent vehicle pocketing. Nevertheless, based on a visual examination of the simulation results, some CMs were expected to have a greater influence on reducing the risk of vehicle pocketing. It is assumed that the method for detecting vehicle pocketing still has room for improvement.

The loadings in the guardrails were assessed by measuring the tensile forces acting along the upper and lower guardrails. Based on the force values obtained, a trend of how each CM influenced the force distribution could be derived. However, this approach does not provide any indication of material failure. The bending of the guardrails around the face of the connection element, which was observed in some variations, was identified as a source of high stress on the material that could lead to material failure. In order to properly identify such critical loads in the simulation, local strain values of the guardrail need to be measured and evaluated. Moreover, this should be preceded by detailed validation of the guardrail at the component level to ensure reliable results. However, the results on a tensile force basis facilitated a simple but effective assessment method to identify the influences of each CM.

It can be stated that some CMs not only influence the analyzed criteria in a positive way. While the values for some criteria decrease, increases in other criteria can occur. For example, CM3 (lateral offset of the first concrete elements) results in decreases in the working width and tensile force in the lower guardrail, but causes an increase in the tensile force in the upper guardrail. Nevertheless, implementation of CM3 is necessary due to its positive effects. However, its negative effects are offset by the implementation of other CMs. Thus, the implementation of all described CMs is necessary to provide the functionality of the TC investigated here and decrease the risk of penetration and vehicle pocketing significantly.

All CMs are designed in a way that standard parts of the connected base RRS can be used to set up the TC. This characteristic facilitates the application of the CMs to other RRS combinations as well.

The functionality of the base TC and the variations in the parameter study were analyzed at impact location B. The findings from this study are, therefore, based on the results of a vehicle impact at this exact impact location. The investigation into further impact locations outside the area over which the three analyzed impact locations extend (i.e., shifting the impact location further in the direction of the two basis RRSs) does not provide any additional knowledge. The risk of vehicle pocketing is observed to be the greatest for impact location B based on the extent of guardrail deformation. It is assumed that for all other impact locations, the risk of vehicle pocketing is significantly lower as the vehicle is already deflected by either the steel or concrete RRS. To support this thesis, several impact locations, applicable to the virtual assessment methods B3 and B4 (according to ENV 1317-10) [14], may be simulated and the selected impact location can be verified as the most critical. The complexity of identifying the most critical impact location in correlation with the norm has also been reported in other studies [16].

This study highlights the benefits of using FE simulations. Numerous variations can be simulated and evaluated in a cost-effective manner. FE simulations guarantee identical boundary conditions for all variations, allowing a direct comparison of all results and the identification of isolated influences.

The validated FE model of the TC can be used for further investigations on additional CMs, or for evaluating the restraint functionalities in impact configurations involving other vehicle types.

5. Limitations

Although it was possible to generate knowledge based on the simulations carried out, the results obtained are subject to some limitations.

The influence of the construction measurements was analyzed based on the simulation of the TB61 impact on a TC, combining RRSs with containment levels H3 and H4b. As it was possible to gain insight into the effect on restraint performance in terms of penetration and vehicle pocketing, no conclusions can be drawn about impact severity. For this purpose, simulations with passenger cars have to be performed and evaluated.

Each constructive measure was analyzed on an isolated basis, which means the influence of the implementation of two or more CMs was not investigated. Further insight into the interference of diverse CMs may be achieved by combining several measures.

The applicability of the derived measures to combinations of other systems can only be stated on a theoretical basis. As only components from the two combined RRSs came into use in the TC, the effective implementation of the measures in TCs connecting other RRSs is also assumed to be realizable. The extent to which the individual measures influence the restraint functionality must be derived separately from other RRS combinations.

The parameter study was conducted with an FE model of one specific heavy goods vehicle. This model represents one specific type in terms of geometry and stiffness properties. However, heavy goods vehicles can be found in various designs and types of driving on European roads. The extent to which the results discussed here apply to heavy goods vehicles of different types or with different structural stiffness cannot be stated.

6. Conclusions

The functionality of the TC with the derived restraint principles implemented was confirmed through simulation and testing of a TB61 impact configuration. The developed TC served as the basis for investigating various CMs, which are applicable to diverse in-service TCs on Austrian roads.

This study revealed the isolated influence of each constructive measure implemented, with the combination of all CMs proving to be the optimum. The technical feasibility of the measures as part of a refurbishment of in-service TCs must be determined for each individual TC separately. As in-service TCs are mostly unique constructions fitted to local boundary conditions, the appropriateness and necessity of the measures to be implemented may vary on a case-by-case basis and must be judged by an expert. Nevertheless, this study provides basic knowledge about the principles of operations of the investigated CMs and can be used as a reference in case of uncertainties or during the development phase of new TCs to be certified.

Author Contributions: Conceptualization, E.T.; methodology, E.T. and D.K.; validation, D.K., C.M., M.J., A.B. and O.J.; software, D.K.; formal analysis, D.K.; investigation, D.K., C.M., M.J., A.B. and O.J.; resources, C.M., M.J., A.B. and O.J.; data curation, D.K.; writing—original draft preparation, D.K.; writing—review and editing, E.T., C.M., M.J., A.B., O.J., J.H. and K.G.; visualization, D.K.; supervision, E.T.; project administration, E.T.; funding acquisition, E.T., C.M. and A.B. All authors have read and agreed to the published version of the manuscript.

Funding: This research was funded by the Austrian Research Promotion Agency (FFG) "Mobilität der Zukunft, Ausschreibung Verkehrsinfrastrukturforschung 2020" tender grant number 886159.

Data Availability Statement: Data are contained within the article.

Acknowledgments: The authors would like to acknowledge the use of High-Performance Cluster resources provided by the ZID (IT services) at Graz University of Technology, Austria. Open Access Funding by the Graz University of Technology.

Conflicts of Interest: Author Johann Horvatits is employed at the Federal Ministry for Climate Action, Environment, Energy, Mobility, Innovation and Technology (BMK). Karl Gragger is employed at the Autobahnen- und Schnellstraßen-Finanzierungs-Aktiengesellschaft. The remaining authors declare that the research was conducted in the absence of any commercial or financial relationships that could be construed as a potential conflict of interest.

References

1. European Commission. *Collision Matrix: Road Traffic Fatalities in the EU in 2021*; European Commission/Directorate General Mobility and Transport: Brussels, Belgium, 2023.
2. European Commission. *Facts and Figures Single Vehicle Crashes*; European Commission/Directorate General Mobility and Transport: Brussels, Belgium, 2023.
3. Sternlund, S.; Strandroth, J.; Rizzi, M.; Lie, A.; Tingvall, C. The effectiveness of lane departure warning systems-A reduction in real-world passenger car injury crashes. *Traffic Inj. Prev.* **2017**, *18*, 225–229. [CrossRef] [PubMed]
4. Dean, M.E.; Riexinger, L.E. Estimating the Real-World Benefits of Lane Departure Warning and Lane Keeping Assist. In Proceedings of the WCX SAE World Congress Experience, Detroit, MI, USA, 5–7 April 2022.
5. Utriainen, R.; Pollanen, M.; Liimatainen, H. The Safety Potential of Lane Keeping Assistance and Possible Actions to Improve the Potential. *IEEE Trans. Intell. Veh.* **2020**, *5*, 556–564. [CrossRef]
6. lfD Allensbach. Anzahl der Personen in Deutschland, deren Pkw mit einem Spurhalteassistent Ausgestattet ist, von 2019 bis 2023. Available online: https://de.statista.com/statistik/daten/studie/269289/umfrage/ausstattung-des-pkw-spurhalteassistent/ (accessed on 14 June 2024).
7. KBA. Fahrzeugzulassungen (FZ). Bestand an Kraftfahrzeugen und Kraftfahrzeuganhängern nach Bundesländern, Fahrzeugklassen und ausgewählten Merkmalen. Available online: https://www.kba.de/DE/Statistik/Fahrzeuge/Bestand/bestand_node.html (accessed on 22 May 2024).
8. Li, H.; Bamminger, N.; Magosi, Z.F.; Feichtinger, C.; Zhao, Y.; Mihalj, T. The Effect of Rainfall and Illumination on Automotive Sensors Detection Performance. *Sustainability* **2023**, *15*, 7260. [CrossRef]
9. Morrissett, A.; Abdelwahed, S. A Review of Non-Lane Road Marking Detection and Recognition. In Proceedings of the 2020 IEEE 23rd International Conference on Intelligent Transportation Systems (ITSC), Rhodes, Greece, 20–23 September 2020.
10. Waykole, S.; Shiwakoti, N.; Stasinopoulos, P. Review on Lane Detection and Tracking Algorithms of Advanced Driver Assistance System. *Sustainability* **2021**, *13*, 11417. [CrossRef]
11. Gitelman, V.; Carmel, R.; Doveh, E.; Pesahov, F.; Hakkert, S. An examination of the effectiveness of a new generation of safety barriers. In Proceedings of the Transport Research Arena 2014, Paris, France, 14–17 April 2014.
12. Martin, J.L.; Mintsa-Eya, C.; Goubel, C. Long-term analysis of the impact of longitudinal barriers on motorway safety. *Accid. Anal. Prev.* **2013**, *59*, 443–451. [CrossRef] [PubMed]
13. *EN 1317-2:2010*; Road Restraint Systems—Part 2: Performance Classes, Impact Test Acceptance Criteria and Test Methods for Safety Barriers Including Vehicle Parapets. European Committee for Standardization: Brussels, Belgium, 2010.
14. *CEN/TR 1317-10:2023*; Road Restraint Systems—Part 10: Assessment Methods and Design Guidelines for Transitions, Terminal and Crash Cushion Connection—Transitions. European Committee for Standardization: Brussels, Belgium, 2023.
15. Einsatzfreigabeliste von Fahrzeuge-Rückhaltesystemen. Available online: https://www.bmk.gv.at/themen/verkehr/strasse/infrastruktur/verkehrstechnik/rueckhalt.html (accessed on 24 July 2023).
16. Pajouh, M.A.; Bielenberg, R.W.; Reid, J.D.; Schmidt, J.D.; Faller, R.K.; Emerson, E. Development of Transition between Free-Standing and Reduced-Deflection Portable Concrete Barriers. *Transp. Res. Rec.* **2018**, *2672*, 118–129. [CrossRef]
17. Loprencipe, G.; Moretti, L.; Cantisani, G.; Minati, P. Prioritization methodology for roadside and guardrail improvement: Quantitative calculation of safety level and optimization of resources allocation. *J. Traffic Transp. Eng.* **2018**, *5*, 348–360. [CrossRef]
18. Budzynski, M.; Jamroz, K.; Wilde, K.; Witkowski, W.; Jelinski, L.; Bruski, D. The role of numerical tests in assessing road restraint system functionality. *Eur. Transp. Res. Rev.* **2020**, *12*, 4209. [CrossRef]
19. Fernández, M.A.; García-Escudero, L.Á.; Molinero, A. Analysis of real crashes against metal roadside barriers. *PLoS ONE* **2019**, *14*, e0211674. [CrossRef] [PubMed]
20. Neves, R.R.; Fransplass, H.; Langseth, M.; Driemeier, L.; Alves, M. Performance of some basic types of road barriers subjected to the collision of a light vehicle. *J. Braz. Soc. Mech. Sci. Eng.* **2018**, *40*, 71. [CrossRef]
21. Klasztorny, M.; Nycz, D.; Dziewulski, P.; Gieleta, R.; Stankiewicz, M.; Zielonka, K. Numerical Modelling of Post-Ground Subsystem in Road Safety Barrier Crash Tests. *Eng. Trans.* **2019**, *67*, 513–534.
22. *EN 16303:2020*; Road Restraint Systems—Validation and Verification Process for the Use of Virtual Testing in Crash Testing Against Vehicle Restraint System. European Committee for Standardization: Brussels, Belgium, 2020.
23. NCAC Crash Simulation Vehicle Models. Available online: http://www.ncac.gwu.edu/vml/models.html (accessed on 28 September 2013).